npj | clean water

www.nature.com/npjcleanwater

ARTICLE OPEN

Check for updates

Selected physical and chemical cleanings remove biofilm in seawater membrane distillation without causing pore wetting

Najat A. Amin[1], Harun Elcik[1], Alla Alpatova[1], Graciela Gonzalez-Gil[1], Bastiaan Blankert[1], Nadia Farhat[1], Johannes S. Vrouwenvelder[1,2] and Noreddine Ghaffour[1,2]✉

Membrane distillation (MD) is an emerging process with a proven ability to recover freshwater from streams with a wide range of salinities. However, MD is susceptible to biofouling. This study explores the efficiency of different cleaning strategies in biofilm removal during seawater MD. Hydraulic cleaning and chemical cleanings with 0.3%w w^{-1} ethylenediaminetetraacetic acid (EDTA), 0.3%w w^{-1} NaOCl, and 3%w w^{-1} citric acid were tested. The results showed that permeate flux recovery increased in the order of hydraulic cleaning <3%w w^{-1} citric acid <0.3%w w^{-1} NaOCl ≈0.3%w w^{-1} EDTA. Membrane cleanings substantially reduced the thickness of the residual biofilm layer and decreased its bacterial concentration and resistance to vapor pressure. The post-cleaning permeate conductivities were low suggesting that employed cleaning protocols did not cause pore wetting of hydrophobic polytetrafluoroethylene microporous (0.22 µm) membrane, and membrane rejection properties remained stable.

npj Clean Water (2023)6:61 ; https://doi.org/10.1038/s41545-023-00278-2

INTRODUCTION

Membrane distillation (MD), a thermally driven separation technology, has been actively explored in an array of water treatment applications, ranging from seawater desalination to wastewater reclamation and brine management[1–3]. Even though the history of MD includes several decades, it has been shadowed by conventional desalination mainly due to low oil and gas costs making them more affordable options. However, due to continuous increases in oil and gas prices and their potential depletion, conventional desalination, like multi-stage flash and multi-effect distillation, is becoming costly, necessitating the development of alternative desalination technologies that could overcome the limitations of existing seawater desalination plants.

In MD, the heated saline stream is brought in contact with a hydrophobic microporous membrane, and water vapor evaporates at the membrane surface interface through the dry membrane pores and condenses on the permeate side[4]. At the same time, capillary forces prevent hydrophilic liquids from entering membrane pores[5]. The MD advantages include compactness, lower operating temperatures, ambient operating pressures, utilization of renewable and low-grade energy sources, lower pretreatment requirements, high ions rejection, and little reliance on feed salinity[6,7]. Given these advantages, the MD process could contribute to global water sustainability as an affordable desalination technology by using low-grade energy sources, especially in arid and semi-arid coastal areas that experience water draughts and lack of inland freshwater basins.

Membrane fouling is an intricate phenomenon described as the accumulation, adsorption, or precipitation of the feed water constituents on the membrane surface or within its pores[8,9] that substantially obstructs the performance of MD systems. Membrane fouling causes permeate flux decline, high energy consumption, pore wetting, and poor permeate quality[10,11]. Among different fouling types, biofouling is one of the most severe and pervasive fouling[12–14]. The biofilm emerges by forming a conditioning film on a membrane surface that comprises a range of organic compounds, followed by the attachment of microbial cells or clusters cemented by extracellular polymeric substances (EPS). Finally, a multilayered ripe biofilm structure consisting of live and dead cells trapped in the EPS matrix is formed[15].

Biofouling severity is determined by operating conditions and a microbial consortium of particular feed water[16–18]. Previous studies suggested that operating the MD system beyond the optimal bacteria growth temperatures induced heat stress that results in excessive EPS release[19] and cell apoptosis and aggravation of the organic fouling/scaling[20,21]. These factors exacerbated biofouling and congested permeate flux. Recently, extensive biofilm development and up to 79% of permeate flux decline in the MD process utilizing Red Sea water, i.e., in conditions of high tolerance of marine microorganisms to elevated feed temperatures, was reported[22]. A significant microbial community succession that influenced biofilm structure with increased MD operating time was reported[23]. Strong interactions between the dominant flagella-like cells might solidify the adherence of microorganisms to the membrane surface and consolidate the foulants present on the MD membrane surface by constructing a cobweb-like structure, which substantially aggravates biofouling[18].

Since biofouling of MD systems is inevitable, developing effective membrane cleaning strategies is needed to minimize biofilm growth, maintain stable permeate flux, and ensure the high quality of produced water. Membrane cleaning is differentiated into physical cleaning which removes reversible fouling, and chemical cleaning which eliminates foulants attached to membrane surface through chemical bonding[24]. The high frequency permeate or chemically-enhance backwash[25] that constantly disrupts biomass deposition and hence prevents biofilm formation in ultrafiltration (UF), if applied in MD, would result in membrane pores filled with backwash liquid necessitating additional drying step to cure pore wetting. Alternatively,

[1]Water Desalination and Reuse Center (WDRC), Biological and Environmental Science and Engineering (BESE) Division, King Abdullah University of Science and Technology (KAUST), Thuwal 23955-6900, Saudi Arabia. [2]Environmental Science and Engineering Program, Biological and Environmental Science and Engineering (BESE) Division, King Abdullah University of Science and Technology (KAUST), Thuwal 23955-6900, Saudi Arabia. ✉email: noreddine.ghaffour@kaust.edu.sa

several studies explored the air backwash to recharge the air at the air-liquid interface and remove the liquid from the membrane pores[26,27]. However, its efficiency was greatly reduced in conditions of high feed water salinity due to a substantial lowering of the liquid entry pressure of the dried membranes, making this cleaning method not applicable in brine treatment.

Chemical cleaning is required to control biofilm occurrence in commercial reverse osmosis (RO)[28,29] and UF modules[25]. Despite a cohort of studies that tackle membrane scaling and pore wetting, biofouling control in MD has received little attention. Apparently, the latter is of equal importance to MD systems as biofilm development could deteriorate permeate flux. Despite this, the available literature is still scarce. A sequence of NaOH at pH ~12 and 40 °C, 70% ethanol, and vacuum drying was applied to destroy bacterial deposits and recycle the membrane in subsequent MD experiments[30]. A sequence of increasing concentrations of HCl solutions was applied to extract biofilm from the membrane surface and analyze its chemical composition[18]. However, to the best of our knowledge, biofouling alleviation in MD has not been the primary scope of any biofouling-related studies.

As a step forward to establish MD as a sustainable desalination technology, it is paramount to investigate the removal of biofilms from MD membranes. This exploration becomes particularly crucial when considering its potential application for the desalination of warm coastal seawaters like those in the Middle East. Seawater from the Red Sea often harbors thermophilic bacterial spores and well-adapted mesophilic microorganisms that cause excessive biofilm growth on MD membranes when the feed water temperatures are raised from 45 °C to 65 °C[22]. The proliferation of those heat-tolerant microorganisms causing biofouling has been largely overlooked in the past because the majority of previously reported MD studies utilized natural waters from moderate climates, which typically contain bacteria with lower temperature adaptability[20,23,31]. Furthermore, the architecture of biofilms that grow in MD systems would diverge from those grown in RO systems due to different hydrodynamic conditions and applied pressures. For example, changes in fluid velocity and corresponding shear stress at the membrane surface would impose a substantial effect on biofilm microscopic structure and 3D morphology[32]. A slow flow, typical in MD, would favor the growth of microorganisms in a vertical direction[32], and as previously demonstrated, thick biofilms formed on membrane surfaces in temperature-driven MD processes were more porous (or less compact) than those developed in pressurized RO systems. As such, disrupting the structure of biofilms that grow in MD systems could require distinct cleaning approaches. However, comprehensive biofilm elimination strategies in MD are still lacking. Therefore, the objective of this study was to systematically examine and compare the effect of four selected physical and chemical cleaning methods on biofouling removal during the direct contact membrane distillation (DCMD) process utilizing real Red Sea water, an essential source of desalinated water in MENA countries[33,34]. The selection of cleaning protocols used in this study was based on several considerations. Given that biofilms formed in the MD process have a loose structure[20], we expected that alteration of system hydrodynamic conditions could aid in their detachment from the membrane surface. Second, we considered recommendations of commercial membrane module manufacturers with respect to chemicals used for mitigating organic and biofouling in RO and UF systems but adjusted them. For example, it is critically important for the MD membrane to retain its hydrophobicity which could be altered upon its contact with surfactants used in different cleaning formulations[25,28,35]. Our recent study[36] showed that sodium dodecyl sulfate, recommended as a primary formulation to control biofilm growth in commercial RO elements[28], caused pore wetting and process shutdown in MD. As such, the prospective cleaning formulations in MD should not induce pore wetting, and only those that will not change permeate conductivity after membrane cleaning should be adopted. Third, we considered the specific chemistry of the Red Sea water which is ubiquitous in Ca^{2+} ions[34] that are known for aggravating organic fouling on a membrane surface[37].

Based on these considerations, we selected four different cleaning methods, hydraulic cleaning at elevated feed flow velocity, and chemical cleanings with 0.3%w w^{-1} EDTA, 0.3% w w^{-1} NaOCl, and 3%w w^{-1} citric acid. The EDTA, a strong chelating agent[38], is recommended for biofouling removal by DuPont[25,28] and Hydranautics[29]. NaOCl, a potent bacteriocide, is suggested for chemically enhanced backwash and cleaning in place of polyvinylidene fluoride UF modules in seawater pretreatment[25]. Citric acid is a mild chelating agent in a pH range of 4–8[39] that is also used to clean commercial UF and RO membrane modules[25,28,29]. Importantly, all three formulations have previously been utilized in MD cleaning tests[40–42].

The biofilm development experiments were conducted at 55 °C for three days (72 h) to allow for the development of mature biofilm and were followed by membrane cleaning. Permeate flux recovery and changes in vapor pressure biofilm resistances before and after membrane cleaning were estimated for each cleaning type. In situ optical coherence tomography (OCT) was used to monitor biofilm development on the membrane surface and assess the efficiency of biomass removal. The biofilm compositions before and after cleanings were analyzed by the flow cytometry (FCM) and three-dimensional fluorescence excitation-emission matrix (3D-FEEM), respectively. The conductivity of the permeate stream was monitored to evaluate the effect of membrane cleanings on pore wettability and membrane integrity. We found that cleaning protocols utilized in this study effectively removed bacteria and biofilm organic constituents from the membrane surface. The applied cleaning strategies facilitated high permeate flux recovery and a considerable reduction in biofilm thickness and vapor flux resistance. Importantly, all tested cleaning protocols have not compromised membrane rejection properties and permeate conductivity.

RESULTS AND DISCUSSION

Red Sea bacteria adapted to high DCMD operating temperature

We assessed changes in bacterial cell concentration in the feed water as a function of DCMD operating time (Fig. 1). The initial bacterial concentration in the feed was $1.7 \times 10^8 \pm 8.5 \times 10^6$ cells mL^{-1} and after 48 h of DCMD, the total number of cells duplicated and reached $3.7 \times 10^8 \pm 1.8 \times 10^7$ cells mL^{-1}. At this phase, the growth rate of bacteria slowed down due to nutrient depletion and the accumulation of toxic waste products[43]. At the end of 72 h, the total number of bacterial cells slightly decreased and reached $3.1 \times 10^8 \pm 1.5 \times 10^7$ cells mL^{-1}. The intact cells dominated the damaged cells over the entire DCMD process, albeit their number declined at the end of the biofouling experiment. Consistently with previous observations[22], this finding confirmed the good adaptability of the Red Sea water microbes (both mesophilic and thermophilic) to high MD feed water temperatures.

Biofilm development on membrane surface caused flux decline

The DCMD system was operated for 72 h to achieve a substantial biofilm layer on a membrane surface. Each fouling experiment was run in parallel and was followed by one of the membrane cleanings (hydraulic or chemical). As seen in Fig. 2, fouling experiments were reproducible, allowing to compare different cleaning methods in conditions of fouled membrane surfaces. Permeate flux decline of 75% (from 32 ± 1.6 L m^{-2} h^{-1} to 8 ± 0.5 L m^{-2} h^{-1}) indicated a substantial effect of biofilm on

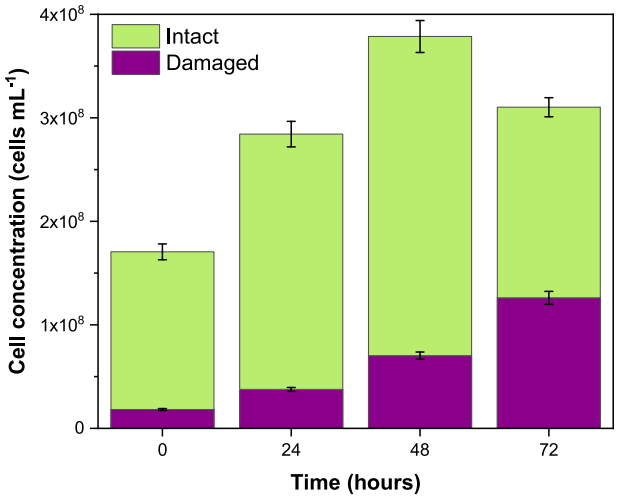

Fig. 1 Bacterial cell concentration in the feed water as a function of operating time during the direct contact membrane distillation (DCMD). Feed water temperature was set to 55 °C. Each DCMD experiment was duplicated, and bacterial cell concentrations are presented as mean values ± standard deviations.

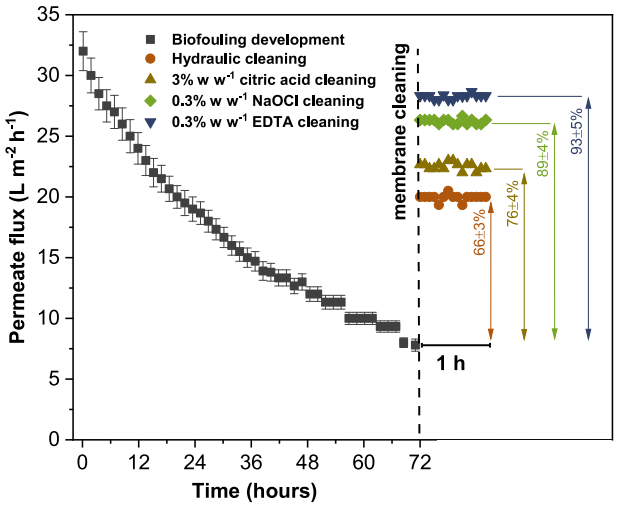

Fig. 2 Permeate flux decline during biofilm development in direct contact membrane distillation (DCMD) and permeate flux recovery after different membrane cleanings. Operating conditions: feed and permeate temperatures were set to 55 °C and 20 °C, respectively, and feed and permeate linear flow velocities were set to 0.28 m s^{-1} and 0.14 m s^{-1}, respectively. Each DCMD experiment was duplicated, and permeate fluxes are presented as mean values ± standard deviations.

DCMD process performance. Figure 3a shows the cross-sectional OCT images of biofilms that developed on the membrane surface as a function of DCMD operating time. A significantly lower increase in biofilm thickness (20 ± 10 µm) was recorded in the initial 24 h of DCMD as compared to its steep increase to 85 ± 15 µm and 175 ± 30 µm after 48 h and 72 h of operations, respectively, due to bacterial proliferation and EPS secretion[16]. Development of a conditioning layer by precipitation of organic feed water constituents[44], and deposition of bacteria[30] that are brought to the membrane surface by tangential flow would narrow or block the membrane pores, thereby creating mass-transfer resistance that sharply deteriorated permeate flux at the beginning of the DCMD process.

To evaluate biofilm fouling mechanisms at different DCMD stages, we plotted graphs that corresponded to four classical fouling models (cake filtration, complete, standard, or intermediate pore blockings) at 12 h, 36 h, and 72 h of the DCMD process (Fig. 4) that corresponded to initial DCMD, middle, and end of the DCMD process, respectively. While a good relationship between the model parameters with high R^2 values was found after 12 h of DCMD (Fig. 4a–d), a phenomenon that is associated with the biofilm formation and is not considered in the classical models, started playing a role with the increase in operating time at 36 h (Fig. 4e–h) and 72 h (Fig. 4i–l). This finding can be explained as follows. One of the assumptions of the classical fouling models is that membrane fouling is caused by the precipitation of the particles from the feed water[45,46]. As such, the formation of the conditioning layer on the membrane surface in the initial DCMD stage (i.e., at 12 h) as a result of organics precipitation is sufficiently described by classical fouling models. Although R^2 values of all four models were close to each other, the OCT images revealed the formation of a fouling layer on the membrane surface. As such, we suggest that the initial stage of biofilm development is likely dominated by the cake filtration mechanism ($R^2 = 0.9861$), along with pore-blocking which also contributes to pore narrowing ($R^2 = 0.9884$). As DCMD evolves, a thicker biofilm layer is formed (Fig. 3a), causing further permeate flux decline (Fig. 2). A maturation of biofilm leads to EPS release and multiplication of microbial cells directly on the membrane surface, thereby halting the condition of particle precipitation from the feed water as the sole fouling cause. As a result, the model fitting at 36 h and 72 h deteriorated as compared to that observed at 12 h, implying that classical models could not any more describe the membrane fouling mechanisms. In summary, biofilm development on a membrane surface caused a substantial decline in permeate flux. However, the applied classical fouling models were able to adequately describe the membrane fouling mechanisms only at the beginning of biofouling experiments and lost their validity with the increase in DCMD operating time.

Flux recovery was governed by the type of membrane cleaning

Monitoring changes in permeate flux before and after membrane cleaning is considered a common method of assessing cleaning efficiency that allows for a direct evaluation of the biofilm removal potential of different cleaning protocols. We estimated permeate flux recoveries after membranes were cleaned by hydraulic cleaning with Milli-Q water and by different chemical solutions. As seen in Fig. 2, the efficiency of permeate flux recovery increased in the order of hydraulic cleaning <3%w w^{-1} citric acid <0.3%w w^{-1} NaOCl ≈ 0.3%w w^{-1} EDTA. Although the efficiency of hydraulic cleaning was lower than that of chemical cleanings, it was capable of removing a substantial part of biofouling, thereby restoring 66 ± 3% of the initial permeate flux. We suggest that the loose structure of MD biofilm[22] would ease its detachment from the membrane surface under high shear stress conditions. Another factor that may improve the efficiency of hydraulic cleaning is the low phosphorous concentration in the Red Sea water. Thus biofilm that developed on a membrane surface utilizing Red Sea water was readily peeled off the RO membrane surface during the hydraulic cleaning compared to a biofilm that grew from the feed water with twice higher phosphorous concentration[47]. The observed effect was attributed to reduced cohesive forces of biofilms that developed under phosphorous-limited conditions of the Red Sea water facilitating their detachment from the membrane surface.

When comparing permeate flux recoveries after applying different chemical cleaning solutions, it is clear that the type of chemical formulation determines membrane cleaning efficiency. While membrane cleanings with 0.3%w/w EDTA and 0.3%w/w

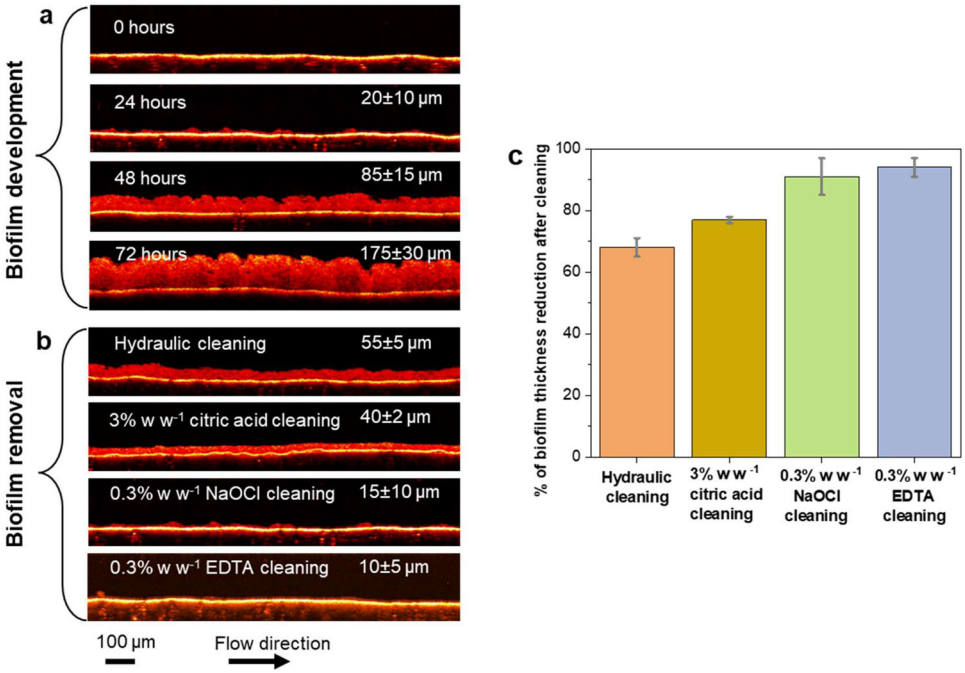

Fig. 3 Effect of membrane cleaning on biofilm development on the membrane surface. Cross-sectional optical coherence tomography (OCT) images of biofilms developed on membrane surface at different operating times (**a**); cross-sectional OCT images of the residual biofilm after different membrane cleanings (**b**); and percent (%) of biofilm thickness reduction after different membrane cleanings (**c**). Operating conditions: feed and permeate temperatures were set to 55 °C and 20 °C, respectively, and feed and permeate linear flow velocities were set to 0.28 m s^{-1} and 0.14 m s^{-1}, respectively. Each DCMD experiment was duplicated, and biofilm thicknesses are presented as mean values ± standard deviations. The scale bar is shown in the top image (0 h) and is the same for all images. The scale bar corresponds to 100 µm.

NaOCl exhibited high permeate flux recoveries (93 ± 5% and 89 ± 4%, respectively), 3%w w^{-1} citric acid was less successful, providing 76 ± 4% of permeate flux recovery. The high performance of 0.3%w w^{-1} EDTA could be attributed to its high potential to break down the intermolecular bridges between the organic foulants or foulants and the membrane surface[48,49]. As known, Ca^{2+} ions that are abundant in the Red Sea water[34] could react with acidic groups of hydrophilic organics to form a cross-linked gel layer that aggravates membrane fouling and deteriorates permeate flux[50,51]. The EDTA molecule forms strong complexes with divalent cations due to its strong chelating abilities, especially in alkaline conditions when its carboxylic groups are deprotonated[52]. As such, the EDTA could replace organic molecules in their complexes with Ca^{2+} via the ligand exchange leading to a rupture and detachment of biofilm structure from the membrane surface.

The NaOCl is a potent chemical with a proven ability to alleviate biofouling through oxidation and breaking down biopolymers to more hydrophilic compounds by imparting them functional groups with a higher oxygen content that reduces biofilm adhesion to the membrane surface[53]. In addition, NaOCl can disintegrate microbial flocs into soluble organic materials and fine particulates that accelerate the oxidation process[54]. The lower cleaning efficiency of 3%w/w citric acid observed in our study could be attributed to the complex composition of the biofilm layer comprised of different microbial species and EPS components that may impede its permeation through the biofilm. Similarly, the cleaning potential of citric acid in biofilm removal was reduced with increasing complexity and diversity of microorganisms that constituted biofilm[55]. Another factor that adversely affects the cleaning efficiency of citric acid is the lower stability constants between the citric acid and Ca^{2+}, Mg^{2+}, and other metals compared to those of EDTA[56], making citric acid of low efficiency in breaking down biofilm structure.

In summary, hydraulic cleaning succeeded in restoring permeate flux due to lost biofilm architecture and reduced cohesive forces. Despite different biofilm removal mechanisms, 0.3w w^{-1} EDTA and 0.3w w^{-1} NaOCl achieved superior cleaning efficiencies, substantially improving permeate flux. It is also important to note that, unlike the RO process, which requires extensive feed water pretreatment[46], the MD process is less demanding in terms of feed water quality. In this study, the seawater was directly supplied from the Red Sea through the offshore pipeline and was immediately used in DCMD experiments. However, as evidenced by the results of this study, biofilm removal was very effective in no-feed pretreatment conditions.

Effect of membrane cleaning on biofilm structure

The thickness of residual biofilm was reduced due to cleanings. We further evaluated the OCT images of the residual biofilm that remained on the membrane surface after different membrane cleaning types. As shown in Fig. 3b, the residual biofilm thickness followed the order of: 0.3%w w^{-1} NaOCl < 0.3%w w^{-1} EDTA < 3% w w^{-1} citric acid < hydraulic cleaning. Consistently with permeate flux recovery trends, hydraulic cleaning produced the least reduction of biofilm thickness (68 ± 3%), lowering it from 175 ± 30 µm to 55 ± 5 µm. As clearly seen in Fig. 3b, the application of chemical cleaning has decreased biofilm thickness to a greater extent as compared to hydraulic cleaning. The biofilm thicknesses comprised 40 ± 2 µm, 15 ± 10 µm and 10 ± 5 µm for 3%w w^{-1} citric acid, 0.3%w w^{-1} NaOCl and 0.3%w w^{-1} EDTA corresponding to removal efficiencies of 77 ± 1%, 91 ± 6% and 94 ± 3%, respectively (Fig. 3c). Although biofilm removals achieved with 0.3%w w^{-1} NaOCl and 0.3%w w^{-1} EDTA are comparable, the morphology of residual biofilm after its cleaning with 0.3%w/w NaOCl has distinct mushroom-like features as compared to a smoother biofilm layer that was left on a membrane surface after its cleaning with 0.3%w w^{-1} EDTA. A

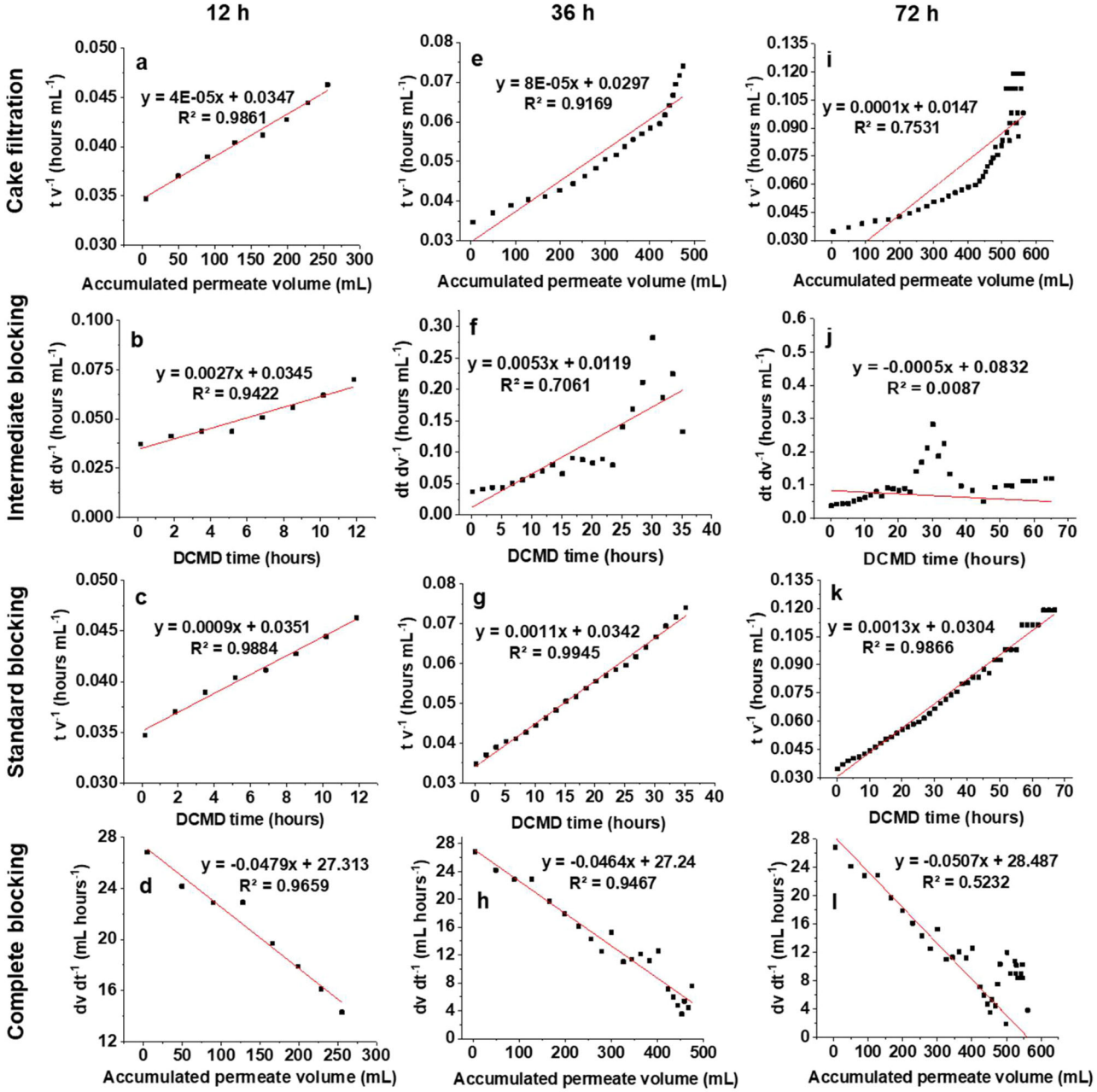

Fig. 4 Fitting of classical fouling models after 12 h, 36 h, and 72 h of direct contact membrane distillation (DCMD). The models describe the following mechanisms: cake filtration (**a**, **e**, **i**), intermediate blocking (**b**, **f**, **j**), standard blocking (**c**, **g**, **k**), and complete blocking (**d**, **h**, **l**).

higher biofilm roughness of a residual biofilm in case 0.3%w w^{-1} NaOCl could imply its higher re-growth potential in subsequent DCMD fouling/cleaning cycles.

As evidenced by permeate recovery (Fig. 2) and biofilm thickness reduction (Fig. 3) trends, the application of lower EDTA and NaOCl doses compared to those recommended by RO and UF manufacturers[28,29], resulted in high-efficiency membrane cleaning. The observed effect could be attributed to the different morphology of biofilms that grow on membrane surfaces in different membrane separation processes. Thus, the looser biofilms that develop on the MD surface without applied pressure[16,20] would allow easier penetration of the cleaning solution. Our findings confirm that although biofilm formation is a common obstacle of all membrane separation processes, its mitigation strategies would be dictated by a process type.

Membrane cleanings reduced bacterial cell concentration

Figure 5 shows the total bacterial cell concentration in biofilms after 72 h of DCMD and after different membrane cleanings. The number of bacterial cells on the membrane surface before the membrane cleanings comprised $1.6 \times 10^9 \pm 7.9 \times 10^7$ w w^{-1} and considerably decreased following cleaning trials. The hydraulic cleaning was the least effective, with a post-cleaning biofilm cell concentration of $5.3 \times 10^8 \pm 2.6 \times 10^7$ cells cm^{-2} and removal efficiency of 67 ± 1%. This was followed by 3% citric acid with the remaining cells concentration of $3.2 \times 10^8 \pm 1.6 \times 10^7$ cells cm^{-2} and removal efficiency of 80 ± 1%. Concurrently, the application of 0.3%w w^{-1} NaOCl and 0.3%w w^{-1} EDTA solutions reduced bacterial cell count by almost two orders of magnitude to $1.4 \times 10^7 \pm 7.2 \times 10^5$ cells cm^{-2} and $1.7 \times 10^7 \pm 8.8 \times 10^5$ cells cm^{-2}, respectively, corresponding to the removal efficiencies of

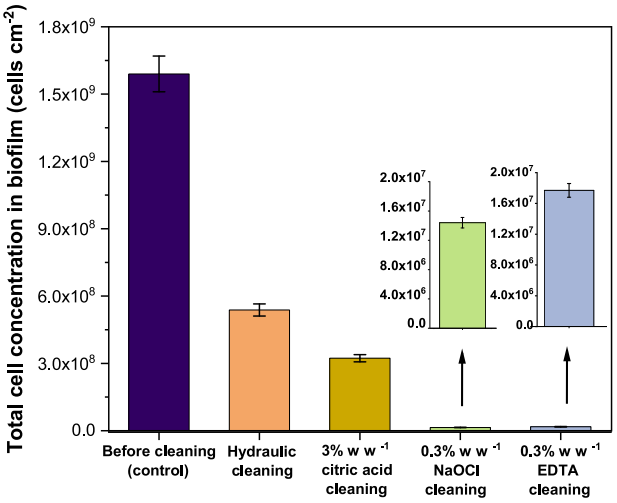

Fig. 5 Total bacterial cell concentrations in biofilm after 72 h of biofilm development in direct contact membrane distillation (DCMD) and in the residual biofilms after application of different membrane cleaning types. Operating conditions: feed and permeate temperatures were set to 55 °C and 20 °C, respectively, and feed and permeate linear flow velocities were set to 0.28 m s^{-1} and 0.14 m s^{-1}, respectively. Each DCMD experiment was duplicated, and bacterial cell concentrations are presented as mean values ± standard deviations.

91 ± 0.2% and 89 ± 0.3%. The lower efficiency of bacterial cell removal observed with hydraulic cleaning compared to chemical cleanings suggests that although slacker biofilm structure eases biofilm removal in conditions of elevated shear stress, chemical interactions between the biofilm components play a significant role in biofilm removal. As such, chemical cleaning would be more effective in eliminating bacterial cells from the MD membrane surface. In addition, bacterial cells that are left on the surface after membrane cleanings could serve as anchors for further membrane surface re-colonization and biofilm build-up.

Cleanings reduced the intensity of organic fluorescent peaks

The 3D-FEEM analysis was carried out to assess the organic compositions of biofilm grown on the membrane surface after 72 h of DCMD and residual biofilms after membrane cleanings. As shown in Fig. 6, four main peaks with different fluorescence intensities were detected after 72 h of DCMD. Two peaks were attributed to proteins, namely peak I (excitation: 250–280 nm, emission: <380 nm) and peak II (excitation: 220–250 nm, emission: 330–380 nm), and the other two peaks were attributed to fulvic acid-like (peak III; excitation: 220–250 nm, emission: >380 nm) and humic acid-like (peak IV; excitation: >280 nm, emission: >380 nm) compounds[57,58]. The intensity of protein peak I in the fluorescence spectrum was the highest, suggesting biofilm maturation and protein release from decayed microbial cells[59]. The protein species play an important role in developing a biofilm layer on the MD membrane due to enhanced interactions between the hydrophobic MD membrane surface and protein molecules[21,60]. This improves protein adhesion and promotes the binding of other water constituents and bacteria products that exacerbate biofilm growth[61].

A significant reduction in fluorescence intensities of all monitored biofilm organic constituents was observed for all cleaning protocols. A comparison of peak intensity corresponding to proteins peak I before and after membrane cleanings revealed that the application of 0.3%w w^{-1} NaOCl and 0.3%w w^{-1} EDTA solutions reduced its intensity by 94%, while hydraulic and 3%w/w citric acid cleanings were less effective, resulting in removal efficiencies of 81% and 84%, respectively. In the case of 0.3% w w^{-1} NaClO, the observed effect can be attributed to the oxidation of intermolecular disulfide bonds of protein molecules trapped in the EPS layer that enhances their solubilization[62]. The EDTA molecules could substitute proteins in their complexes with Ca^{2+} [63], thereby dislodging unconstrained proteins from the membrane surface. It is worth noting that although hydraulic cleaning had lower efficacy than chemical cleaning, a substantial amount of fouling caused by proteins corresponding to region I was reversible and was therefore removed in high shear stress conditions during hydraulic cleaning. The removal of proteins that corresponded to region II was poorer, comprising 58%, 59%, 71%, and 69% for hydraulic cleaning, 3%w/w citric acid, 0.3%w w^{-1} NaOCl and 0.3%w w^{-1} EDTA, respectively.

Application of 0.3% w/w EDTA solution was the most effective in reducing the intensity of the fulvic acid-like (62%) and humic acid-like (79%) compounds through breaking down the "bridges" between the carboxylic groups and Ca^{2+} ions and subsequent disintegration of humic aggregates[37,64]. Oxidation of fulvic acid-like and humic acid-like compounds by 0.3%w w^{-1} NaOCl through the cleavage of aliphatic and aromatic functional groups[65] was less effective (54% and 71%, respectively). A 3%w w^{-1} citric acid was the least successful in dislodging both types of humic compounds (50% and 65%, respectively) due to its acidic pH. Although hydraulic cleaning was less powerful as compared to chemical cleaning (removal efficiencies of 45% and 62% for fulvic acid-like and humic acid-like compounds, respectively), a substantial portion of both humic substances was reversibly attached to the membrane surface. The removal efficiencies of fulvic acid-like compounds were substantially lower as compared to those of humic acid-like compounds, especially in the case of hydraulic cleaning. The observed effect could be attributed to the formation of a more compact fouling layer on the membrane surface in the case of fulvic acids due to their smaller aggregate sizes as compared to humic acids[66], which would be more difficult to remove by increasing the shear stress at the membrane surface.

Our findings indicate that the removal efficiency of tested cleaning formulations was governed by the type of biofilm constituent. While 0.3%w w^{-1} EDTA and 0.3%w w^{-1} NaOCl were closely effective in removing protein material, 0.3%w w^{-1} EDTA had higher potential in eliminating biofilm humic compounds due to its superior complexation properties.

Cleanings did not affect permeate conductivity. In our study, the conductivity of the permeate stream was monitored daily to assess the effect of biofilm development and membrane cleaning on permeate quality. Figure 7 shows changes in permeate conductivities for individual DCMD biofouling experiments conducted in the same operating conditions. Albeit some variations were caused by using different membrane coupons, permeate conductivities increased with increasing operating time and ranged from 30 ± 2 µS cm^{-1} to 39 ± 2 µS cm^{-1} after 72 h of DCMD. Although the final permeate conductivities were low, their increase with the increase in operating time is an indication of the partial pore wetting caused by biofilm development. The increase in the permeate conductivity was more noticeable within the initial 24 h of DCMD due to the formation of a conditioning film that negatively affected surface hydrophobicity and caused the passage of water droplets through the membrane pores 22. The development of a thick biofilm layer suppressed pore wetting as reflected by slowing down the rate of conductivity increase with the increase in operating time.

After 72 h of the biofouling experiment, membrane cleaning was conducted, and the DCMD process was resumed by utilizing 30 g L^{-1} of NaCl to examine its effect on the membrane's integrity and pore wetting. Figure 8 shows that permeate water conductivities measured after 1 h of the DCMD process were not increased for any cleaning type implying that tested cleaning protocols have not caused pore wetting and deterioration of membrane rejection. These results emphasize the importance of developing appropriate

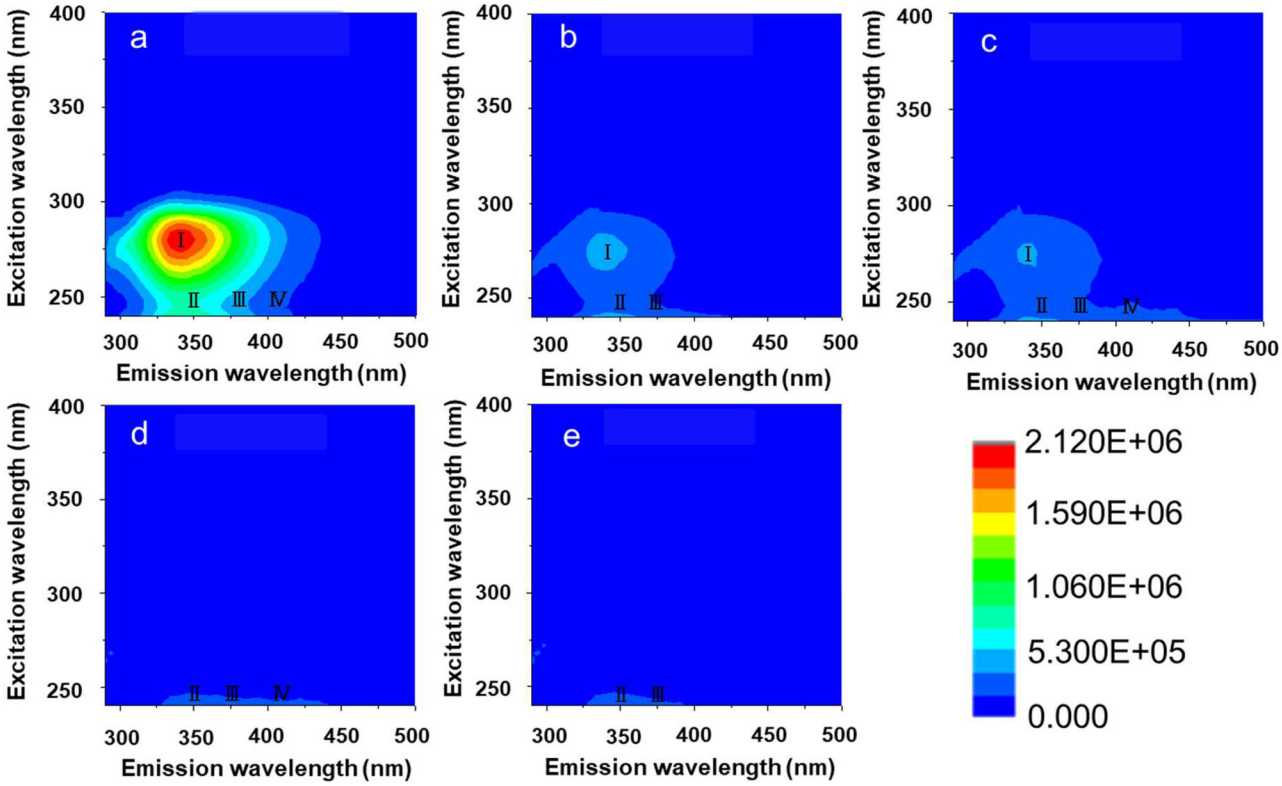

Fig. 6 Fluorescent intensity of biofilms before and after membrane cleanings. Three-dimensional fluorescence excitation-emission matrix (3D-FEEM) contour plots of biofilm organic composition after 72 h of biofilm development in direct contact membrane distillation (DCMD) (**a**), and residual biofilms after hydraulic cleaning (**b**), 3%w w^{-1} citric acid (**c**); 0.3%w w^{-1} NaOCl (**d**), and 0.3%w w^{-1} EDTA (**e**). Four regions were identified: proteins corresponding to peak I, proteins corresponding to peak II, fulvic acid-like compounds corresponding to peak III, and humic acid-like compounds corresponding to peak IV.

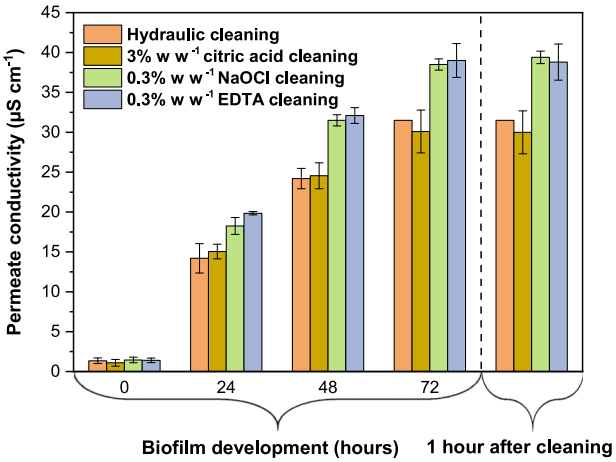

Fig. 7 Changes in permeate conductivities during biofilm development in direct contact membrane distillation (DCMD) and after different membrane cleanings. Operating conditions: feed and permeate temperatures were set to 55 °C and 20 °C, respectively, and feed and permeate linear flow velocities were set to 0.28 m s^{-1} and 0.14 m s^{-1}, respectively. Each DCMD experiment was duplicated, and conductivities are presented as mean values ± standard deviations.

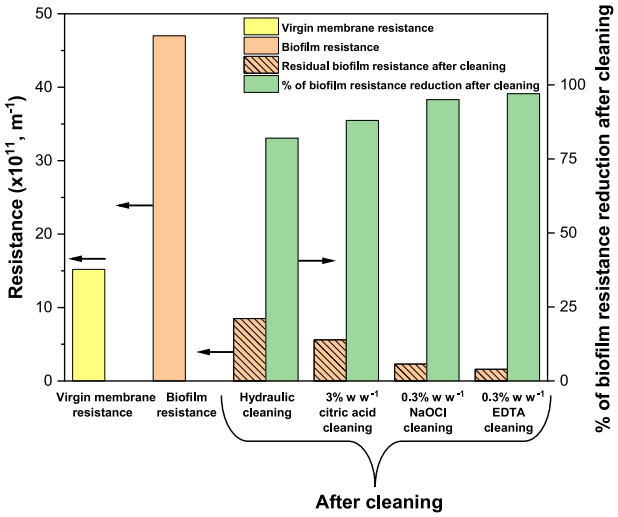

Fig. 8 Effect of membrane cleaning on biofilm resistance to vapor pressure. Solid bars show resistances of virgin membrane, biofilm after 72 h of direct contact membrane distillation (DCMD), and % of biofilm resistance reduction after different membrane cleanings. The dashed bars show residual biofilm resistances after different membrane cleanings.

cleaning protocols that ensure the stable performance of hydrophobic membranes after applied chemical cleanings.

Findings presented in this section suggest profound changes in residual biofilm structures for all cleaning types, including a substantial reduction in the total bacterial cell concentration and intensity of fluorescent peaks that pertained to biofilm organic constituents like protein and humic matter. As a result, the residual biofilm thicknesses substantially decreased as compared to their pre-cleaned values, which allowed for to restoration of permeate flux under each tested operating condition.

Cleanings lowered biofilm resistance to vapor pressure

In MD, evaporation is achieved through the vapor-liquid interface that occurs at the meniscus of the membrane pores[44]. The presence of biofilm on a membrane surface induces the Kelvin effect that, in turn, decreases vapor pressure at a pore entrance[67] and creates additional resistance to vapor flow[44,67]. Given that the driving force of the MD process is the vapor pressure difference across the hydrophobic membrane, the resistance of a biofilm layer that develops on the membrane surface would comprise vapor pressure and hydraulic pressure resistances. Considering the small effect of hydraulic pressure on vapor pressure changes in MD, the contribution of hydraulic resistance to the total biofilm mass-transfer resistance would be minor as compared to that of vapor pressure resistance. Similarly to the RO process where biofilm-induced concentration polarization, rather than hydraulic resistance, is a major factor that affects permeate flux[68,69], biofilm-induced temperature polarization that lowers temperature gradient and reduces vapor flux across the membrane, is likely a major factor that controls vapor transport in MD. Both microbial and EPS biofilm constituents contributed to biofilm resistance in MD. While physical blockage of the membrane pores by bacteria enabled the formation of a stagnant layer over the membrane surface, thereby aggravating temperature polarization and decreasing diffusion to the membrane surface[30], the protein non-porous layer also created additional thermal and hydraulic resistance to the vapor flow[44]. It was suggested that convective transport through the biofilm in the MD process is determined by its porosity[70]. This supports the previous statement that despite its apparently high thickness, biofilms that developed on MD membranes are sparse and provide less obstruction to vapor flow as compared to biofilms that grow in pressurized membrane systems and experience compression of the biofilm gel layer. Furthermore, our recent study that explored mechanisms of the temporal and spatial distribution of biofilms on a surface of MD membrane[22] revealed that the porosity of biofilms was determined by their microbial and EPS contents, with higher EPS concentration and lower bacterial content leading to more compact biofilms compared to looser biofilms that were characterized by a larger number of bacterial cells and lower EPS concentration.

We further assessed the resistance of biofilms to vapor pressure before and after different cleanings (Fig. 8). After 72 h of DCMD, the vapor pressure resistance of biofilm increased three-fold, from $4.7 \times 10^{12}\ m^{-1}$ to $1.52 \times 10^{12}\ m^{-1}$. The vapor pressure resistances were reduced to $8.5 \times 10^{11}\ m^{-1}$, $5.6 \times 10^{11}\ m^{-1}$, $2.3 \times 10^{11}\ m^{-1}$ and $1.6 \times 10^{11}\ m^{-1}$ for hydraulic cleaning, 3%w w^{-1} citric acid, 0.3%w w^{-1} NaOCl and 0.3%w w^{-1} EDTA cleanings, respectively. Consistently with permeate recoveries, the highest reduction of vapor pressure resistances was achieved with 0.3%w w^{-1} EDTA and 0.3%w w^{-1} NaOCl (97% and 95%, respectively), followed by 3%w w^{-1} citric acid (88%) and hydraulic (82%) cleanings.

Goh et al.[67] suggested that both hydrophilic and hydrophobic organic biofilm compounds promoted vapor pressure depression as a result of biofilm development on the MD membrane. Comparing Figs. 6 and 8, we observed a good agreement between the vapor pressure reduction and a decrease in the intensity of the fluorescent-detected biofilm organic compounds. This implies that the removal of organic biofilm fraction is important in tackling MD biofouling and enhancing vapor pressure gradient across the membrane.

We can also expect that the contribution of bacterial cells that are present on a membrane surface to the total biofilm resistance to vapor flow is considerably smaller due to its lower portion in the total biofilm volume and the higher porosity of the bacterial cake layer[22]. This explains high biofilm resistance reductions observed in conditions when a substantial number of bacterial cells are still lingering on the membrane surface after its cleaning (Fig. 5). In summary, although biofilm vapor pressure resistance imposed a substantial effect on DCMD performance, membrane cleaning facilitated its substantial reduction that was well-correlated with the removal of the individual biofilm constituents.

In conclusion, our study explored different biofilm removal techniques during the DCMD process utilizing real Red Sea water. Four physical and chemical cleaning protocols were assessed for their efficiency in eliminating bacterial and organic constituents of biofilms that developed on membrane surfaces and within their pores. Although effective biofouling mitigation strategies have been suggested by commercial RO and UF manufacturers[25,28,29], taking into consideration the high susceptibility of hydrophobic membranes to pore wetting, it was important to explore if membrane rejection properties were adversely impacted after chemical cleaning. The collective data presented in this study suggest that 0.3%w w^{-1} NaOCl and 0.3%w w^{-1} EDTA solutions are the better candidates for biofilm removal in the MD process that achieved the highest degree of permeate flux recovery while maintaining membrane integrity applied cleanings. These chemicals were effective at concentrations lower than those recommended by the common membrane manufacturers making them attractive and affordable options for biofouling mitigation. This is an important finding because, until recently, the majority of MD cleaning studies have been focused on investigating the cleaning potential of inorganic acids in scale removal during the MD process treating synthetic feeds[41], including seawater[71,72] and brines[73,74]. However, as evidenced by the results of this study, 3% w w^{-1} citric acid had limited capacity in biofilm elimination during the DCMD process. Our results also emphasize the importance of developing reliable cleaning protocols that ensure the stable performance of hydrophobic membranes after their contact with harsh chemical environments. The innovative nature of our study suggests that biofouling abatement in MD could successfully be achieved by manipulating common cleaning solutions that are readily available at desalination plants. This would facilitate stable and sustainable performance of the MD process thereby creating grounds for further energy reductions. Besides this, the suggested cleaning techniques could potentially be applicable to any type of MD process making this desalination technology more accessible to industrial and municipal end users. Finally, the findings of this study will aid in developing cost-effective and environmentally friendly cleaning techniques to tackle the issue of membrane biofouling which is unavoidable in membrane processes including MD, thereby assisting in process scale-up and its commercialization.

The major outcomes of this study are as follows:

1. The application of hydraulic cleaning eliminated a substantial part of biomass and restored 66 ± 3% of permeate flux, implying that the loose morphology of biofilm that developed on the MD membrane surface improved the efficiency of hydraulic cleaning. Among tested chemical formulations, 0.3%w w^{-1} NaOCl and 0.3%w w^{-1} EDTA provided the highest permeate flux recoveries of 89 ± 4% and 93 ± 5%, respectively.
2. The thickness of the residual biofilm layer on the membrane surface followed the order of: 0.3%w w^{-1} EDTA < 0.3%w w^{-1} NaOCl < 3%w w^{-1} citric acid < hydraulic cleaning.
3. The 0.3%w w^{-1} NaOCl and 0.3%w w^{-1} EDTA-based cleanings reduced the total cell count on a membrane surface by almost two orders of magnitude. However, a considerable part of microbes remained on a membrane surface, serving as potential anchors for subsequent microbial re-colonization and biofilm build-up.
4. The 3D-FEEM analysis demonstrated that 0.3%w w^{-1} EDTA and 0.3%w w^{-1} NaOCl cleaning solutions achieved the highest removal of all four monitored organic biofilm compounds (protein peaks I and II, humic acid-like and

fulvic acid-like substances).
5. No increase in permeate conductivity was detected for any of the applied cleaning protocols suggesting that membrane rejection was not negatively affected.
6. Given that biofilm development is aggravated with the increase in feed water temperature[22], optimization of active compound concentration is needed to achieve effective membrane cleaning in different temperature conditions.
7. Long-term experiments with an extended number of fouling/cleaning cycles are desirable to explore the effect of residual biofilm accumulation on key membrane properties and the aging of membrane material.
8. A combination of physical and chemical cleanings is also needed to explore to minimize chemical concentration which can put MD in a competitive position with other desalination technologies.
9. Our findings show that although biofilm formation is a common obstacle of all membrane separation processes, its mitigation strategies would be dictated by a process type, conditions in which particular biofouling has been developed, and membrane characteristics.

METHODS

DCMD feed water

The Red Sea water was supplied through the offshore intake pipeline and was used without any further pretreatment. Detailed information on the physicochemical characteristics of the Red Sea water used in this study can be found elsewhere[1]. To escalate the growth of microorganisms, 20 g of Bacto™ Yeast Extract (Becton Dickinson, USA) was dissolved in 5 L of real Red Sea seawater and incubated in a shaking incubator (Model 5000, VWR, USA) at 70 rpm and 30 °C for 24 h. After incubation, the water was diluted with 15 L of fresh Red Sea water to result in 20 L.

DCMD setup and operating protocol

The schematic diagram of the DCMD system is shown in Fig. 9. The DCMD experiments were conducted using a custom-made module with an effective membrane area of 9 cm^2 (6 cm × 1.5 cm). A hydrophobic PTFE microporous membrane with a polyethylene support layer and a nominal pore size of 0.22 µm from Membrane Solutions LLC (China) was utilized in all experiments. Two gear pumps (Model 72211–70, Cole Parmer, USA) were used to circulate the feed and permeate streams in a counter-current mode at linear flow velocities of 0.28 m s^{-1} and 0.14 m s^{-1}, respectively. The lower coolant flow velocity has been chosen to save the pumping energy as our previous study showed less effect of the coolant flow rate on permeate flux as compared to that of the feed flow rate[75]. Temperatures at the feed and permeate sides were set to 55 ± 1°C and 20 ± 1°C, respectively, by employing circulating baths (Model 600-F, Julabo, USA). Permeate conductivities were monitored by using a portable conductivity meter (Cond 3210, WTW, USA) every 24 h. This time interval was found to be sufficient to assess changes in permeate conductivity during DCMD fouling experiments using real Red Sea water[22]. The feed water was continuously stirred by an overhead stirrer (RW 20, IKA, USA) at 250 rpm. The gain in permeate weight was assessed every 10 min using an electronic balance (Model ML3002, Metter Toledo, USA), and the data were logged using LabVIEW (National Instruments, USA). The DCMD experiments were conducted for 72 h in parallel to ensure their reproducibility.

Permeate flux (L m^{-2} h^{-1}) was calculated according to the following equation:

$$J = \frac{W}{\triangle tA} \quad (1)$$

where W is the permeate water gain (L), t is operating time (h), and A is the effective membrane area (m^2).

Membrane cleaning procedure

Hydraulic cleaning. The hydraulic cleaning was conducted by circulating 20 L of Milli-Q water (Advantage A10, Millipore) on the membrane feed side at a linear flow velocity of 0.67 m s^{-1} for 1 h.

Chemical cleaning. The following cleaning formulations were utilized in this study: 3%w w^{-1} citric acid (Sigma-Aldrich, USA), 0.3%w w^{-1} NaOCl (Sigma-Aldrich, USA), and 0.3%w w^{-1} EDTA (Sigma-Aldrich, USA). Concentrations of EDTA, NaOCl, and citric acid were chosen to be within a range of concentrations reported in previous cleaning studies[25,28,29,40–42,48,49,76]. The pH of the EDTA solution was adjusted to 11 by 1 M NaOH (Sigma-Aldrich, USA). A 20 L of cleaning solution was circulated at a flow velocity of 0.28 m/s in the feed loop for 1 h. After this, the feed and permeate

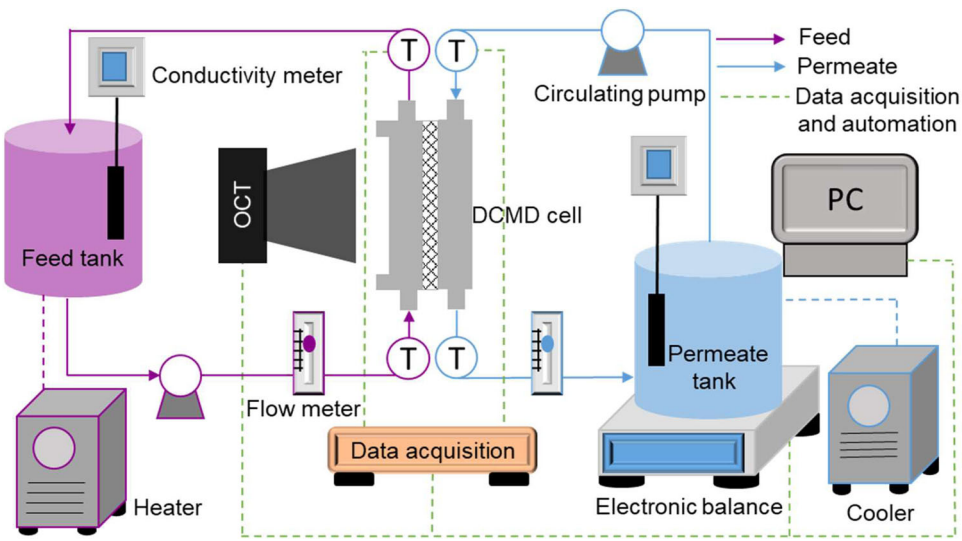

Fig. 9 Schematic diagram of direct contact membrane distillation (DCMD) system. The DCMD system comprised of feed and permeate loops. The feed water was preheated to the desired temperature and supplied to the feed channel of the DCMD module. Water vapor passed through the membrane pores and condensed on the coolant side. The gain in permeate water over the course of DCMD was monitored by the digital balance.

loops were rinsed with 20 L of Milli-Q water at a velocity of 0.28 m s^{-1}. Permeate flux recovery and permeate conductivity changes were evaluated using 20 L of 30 g L^{-1} NaCl (Sigma-Aldrich, USA) at 55 °C for 1 h in the same hydrodynamic conditions as in the biofouling experiment.

Each biofouling/cleaning experiment was conducted in duplicates.

Biofilm characterization

OCT monitoring of membrane surfaces. A spectral-domain OCT device (Ganymede II, Thorlabs, USA) equipped with an LSM03 scan lens was employed for biofilm visualization before and after membrane cleanings. Two-dimensional OCT imaging was carried out at a center wavelength of 930 nm in the middle part of the feed channel with a resolution of 666 pixels × 408 pixels corresponding to 4.0 × 1.2 mm of the membrane area and then processed using Fiji software (National Institute of Health, USA). Biofilm thickness (μm) was calculated by dividing the entire imaged biofilm area over the corresponding biofilm length.

Biofilm extraction procedure. Membrane coupons were removed from the DCMD module and immersed into a 50 mL centrifuge tube. A 10 mL phosphate-buffered saline (PBS) solution was added, and the tube was vortexed (Fisherbrand™ Analog Vortex Mixer, USA) for 2 min, followed by 5 min of sonication in an ultrasonic water bath (5510MTH, Bransonic®, USA). The suspended biomass was used for the FCM and 3D-FEEM analyses.

Flow cytometry analysis. The intact and damaged cells were enumerated by the Accuri C6 Plus FCM (BD Biosciences, USA) using a previously standardized staining protocol[77,78]. Briefly, samples were stained with either SYBR™ Green (SG) (10,000x concentrate, Invitrogen) or SG together with the propidium iodide (PI). The final concentrations of SG and PI in the samples were 1x and 4 μM, respectively. The stained samples were vortexed for 2 s followed by incubation in the dark on a shaking incubator (VWR, Model 3500, USA) at 120 rpm and at 37 °C or 10 min. The samples were loaded on a 96-well plate (Sigma-Aldrich, USA) and 50 μL of each sample was injected into the system at a flow rate of 35 μL min^{-1}. The laser emitting and collecting intensities were set to 488 nm and 533 nm, respectively.

FEEM analysis. Biofilm compositions were analyzed to assess the effectiveness of different cleaning methods on biofilm removal. The formaldehyde-NaOH method developed by Liu and Fang[79] was used to extract biofilms from the membrane surface. The extracted biomasses were treated using 60 μL of 36.5% formaldehyde (Sigma-Aldrich, USA) at 4 °C for 1 h and incubated with 4 mL of 1 M NaOH at 4 °C for 3 h. After treatment, samples were centrifuged (75004521-XT, Thermo Fisher Scientific, USA) at 20,000 rpm for 20 min. The supernatants were filtered through a 0.22 μm filter and dialyzed in a 3500 Da dialysis membrane bag (Thermo Fisher Scientific, USA) for 24 h. The dialyzed samples were lyophilized for 48 h and resuspended in 10 mL of Milli-Q water.

The 3D-FEEM was measured by a Fluoromax-4 spectrofluorometer (Horiba Scientific, Japan). The wavelengths for excitation and emission were 240–400 nm and 290–500 nm, respectively. The photomultiplier tube voltage was set to 700 V, and the scan speed was set to 1500 nm/min.

Membrane and biofilm resistance

The biofilm resistances to vapor pressure were calculated according to a previous study[80]. The vapor pressure (p, Pa) was estimated according to Antoine's equation:

$$p = e^{\left(23.1964 - \frac{38.1644}{T - 46.13}\right)} \quad (2)$$

where T is the absolute temperature (K) of the liquid.

The vapor pressure differences between the feed and permeate sides were calculated by Eq. (3):

$$\triangle\pi = p_f - p_c \quad (3)$$

where $\Delta\pi$ is the vapor pressure difference (Pa), p_f and p_c are the vapor pressures (Pa) on the feed and permeate sides, respectively.

The total resistance (R_T, m^{-1}) consisted of the intrinsic membrane resistance (R_m, m^{-1}) and biofilm resistance to vapor pressure (R_b, m^{-1}).

The resistances were determined as follows:

$$R_T = R_m + R_b \quad (4)$$

$$R_m = \frac{\triangle\pi}{n J_0} \quad (5)$$

$$R_b = \frac{\triangle\pi}{n J_1} - R_m \quad (6)$$

where J_0 is the initial permeate flux (L m^{-2} h^{-1}), J_1 is the permeate flux after biofilm development (L m^{-2} h^{-1}), and n is the dynamic viscosity of water (Pa s).

Fouling models

Four different fouling mechanisms, namely cake filtration (Eq. 7), intermediate blocking (Eq. 8), standard blocking (Eq. 9), and complete blocking (Eq. 10), were used in this study[45,81]. Although classical fouling models were originally developed for constant pressure dead-end filtration with porous membrane, given that the MD process is conducted at a constant driving force with porous membranes, these models have been utilized to assess the fouling behavior of seawater RO reject and ground waters in the air gap MD[82]. In our study, we applied them to explore biofilm fouling mechanisms in MD.

The fouling models are described by the following equations:

$$\text{Cake filtration}: \frac{t}{V} = \frac{1}{J_0}\frac{k_c}{2}V \quad (7)$$

$$\text{Intermediate blocking}: \frac{dt}{dV} = \frac{1}{J_0} - k_i t \quad (8)$$

$$\text{Standard blocking}: \frac{t}{V} = \frac{1}{AJ_0} + \frac{k_s}{2}t \quad (9)$$

$$\text{Complete blocking}: \frac{dV}{dt} = J_0 A - k_b V \quad (10)$$

where J is the permeate flux at any given operating time (L m^{-2} h^{-1}), V is the cumulative permeate volume (L), and the model coefficients are k_c (slope of $\frac{t}{V}$ vs. V), k_i (slope of $\frac{dt}{dV}$ vs. t), k_s (slope of $\frac{t}{V}$ vs. t), and k_b (slope of $\frac{dV}{dt}$ vs. V).

DATA AVAILABILITY

The datasets used and/or analyzed during the current study are available from the corresponding author upon reasonable request.

Received: 16 March 2023; Accepted: 29 August 2023;
Published online: 05 September 2023

REFERENCES

1. Alpatova, A., Alsaadi, A., Alharthi, M., Lee, J.-G. & Ghaffour, N. Co-axial hollow fiber module for air gap membrane distillation. *J. Membr. Sci.* **578**, 172–182 (2019).
2. Sayegh, A., Shylaja Prakash, N., Horn, H. & Saravia, F. Membrane distillation as a second stage treatment of hydrothermal liquefaction wastewater after ultrafiltration. *Sep. Purif. Technol.* **285**, 120379 (2022).

3. Viader, G. et al. Integration of membrane distillation as volume reduction technology for in-land desalination brines management: Pre-treatments and scaling limitations. *J. Environ. Manag.* **289**, 112549 (2021).
4. Lawson, K. W. & Lloyd, D. R. Membrane distillation. *J. Membr. Sci.* **124**, 1–25 (1997).
5. Rezaei, M. et al. Wetting phenomena in membrane distillation: mechanisms, reversal, and prevention. *Water Res.* **139**, 329–352 (2018).
6. Yang, S. et al. Membrane distillation technology for molecular separation: a review on the fouling, wetting and transport phenomena. *J. Mol. Liq.* **349**, 118115 (2022).
7. Ghaffour, N., Soukane, S., Lee, J. G., Kim, Y. & Alpatova, A. Membrane distillation hybrids for water production and energy efficiency enhancement: a critical review. *Appl. Energy* **254**, 113698 (2019).
8. Tijing, L. D. et al. Fouling and its control in membrane distillation—a review. *J. Membr. Sci.* **475**, 215–244 (2015).
9. Soukane, S. et al. Scaling sets the limits of large scale membrane distillation modules for the treatment of high salinity feeds. *J. Clean. Prod.* **287**, 125555 (2021).
10. Elcik, H. et al. Multi-effect distillation brine treatment by membrane distillation: effect of antiscalant and antifoaming agents on membrane performance and scaling control. *Desalination* **493**, 114653 (2020).
11. Mustakeem, M., Qamar, A., Alpatova, A. & Ghaffour, N. Dead-end membrane distillation with localized interfacial heating for sustainable and energy-efficient desalination. *Water Res* **189**, 116584 (2021).
12. Flemming, H.-C. & Wingender, J. The biofilm matrix. *Nat. Rev. Microbiol.* **8**, 623–633 (2010).
13. Flemming, H.-C., Neu, T. R. & Wozniak, D. J. The EPS matrix: the "house of biofilm cells". *J. Bacteriol.* **189**, 7945–7947 (2007).
14. Kerdi, S., Qamar, A., Alpatova, A., Vrouwenvelder, J. S. & Ghaffour, N. Membrane filtration performance enhancement and biofouling mitigation using symmetric spacers with helical filaments. *Desalination* **484**, 114454 (2020).
15. Bar-Zeev, E., Berman-Frank, I., Girshevitz, O. & Berman, T. Revised paradigm of aquatic biofilm formation facilitated by microgel transparent exopolymer particles. *Proc. Natl Acad. Sci.* **109**, 9119–9124 (2012).
16. Bogler, A., Lin, S. & Bar-Zeev, E. Biofouling of membrane distillation, forward osmosis and pressure retarded osmosis: Principles, impacts and future directions. *J. Membr. Sci.* **542**, 378–398 (2017).
17. Jiang, L., Chen, L. & Zhu, L. Fouling process of membrane distillation for seawater desalination: An especial focus on the thermal-effect and concentrating-effect during biofouling. *Desalination* **485**, 114457 (2020).
18. Zheng, L. et al. Insight into the microbial distribution and succession and biofouling mechanism in membrane distillation for desulfurization wastewater treatment. *J. Chem. Eng.* **428**, 131097 (2022).
19. Bogler, A. & Bar-Zeev, E. Membrane distillation biofouling: impact of feedwater temperature on biofilm characteristics and membrane performance. *Environ. Sci. Technol.* **52**, 10019–10029 (2018).
20. Zodrow, K. R., Bar-Zeev, E., Giannetto, M. J. & Elimelech, M. Biofouling and microbial communities in membrane distillation and reverse osmosis. *Environ. Sci. Technol.* **48**, 13155–13164 (2014).
21. Liu, C. et al. The effect of feed temperature on biofouling development on the MD membrane and its relationship with membrane performance: an especial attention to the microbial community succession. *J. Membr. Sci.* **573**, 377–392 (2019).
22. Elcik, H. et al. Elucidating biofouling over thermal and spatial gradients in seawater membrane distillation in hot climatic conditions. *Water Res* **223**, 118983 (2022).
23. Liu, C., Zhu, L. & Chen, L. Biofouling phenomenon of direct contact membrane distillation (DCMD) under two typical operating modes: Open-loop mode and closed-loop mode. *J. Membr. Sci.* **601**, 117952 (2020).
24. Costa, F. C. R. et al. Biofouling in membrane distillation applications—a review. *Desalination* **516**, 115241 (2021).
25. DuPont. *IntegraPac™ Ultrafiltration Module and Skid Product Manual* https://www.dupont.com/content/dam/dupont/amer/us/en/water-solutions/showpad_only/documents/en/UF-IntegraPac-Manual-45-D01776-en.pdf (DuPont 2022).
26. Warsinger, D. M. et al. Reversing membrane wetting in membrane distillation: Comparing dryout to backwashing with pressurized air. *Environ. Sci. Water Res. Technol.* **3**, 930–939 (2017).
27. Warsinger, D. M. et al. Combining air recharging and membrane superhydrophobicity for fouling prevention in membrane distillation. *J. Membr. Sci.* **505**, 241–252 (2016).
28. DuPont. *FilmTec™ Reverse Osmosis Membranes Technical Manual* https://www.dupont.com/content/dam/dupont/amer/us/en/water-solutions/public/documents/en/RO-NF-FilmTec-Manual-45-D01504-en.pdf (DuPont, 2023).
29. Hydranautics. *Technical Service Bulletin. Foulants and Cleaning Procedures for Composite Polyamide RO/NF Membrane Elements, TSB107.27* https://membranes.com/wp-content/uploads/Documents/TSB/TSB107.pdf (Hydranautics, 2020).
30. Krivorot, M., Kushmaro, A., Oren, Y. & Gilron, J. Factors affecting biofilm formation and biofouling in membrane distillation of seawater. *J. Membr. Sci.* **376**, 15–24 (2011).
31. Chen, L., Wang, Y., Chen, Z. & Cai, Z. The fouling layer development on MD membrane for water treatments: An especial focus on the biofouling progress. *Chemosphere* **264**, 128458 (2021).
32. Hartmann, R. et al. Emergence of three-dimensional order and structure in growing biofilms. *Nat. Phys.* **15**, 251–256 (2019).
33. Fortunato, L. et al. Fouling investigation of a full-scale seawater reverse osmosis desalination (SWRO) plant on the Red Sea: membrane autopsy and pretreatment efficiency. *Desalination* **496**, 114536 (2020).
34. Alpatova, A., Alsaadi, A. & Ghaffour, N. Boron evaporation in thermally-driven seawater desalination: Effect of temperature and operating conditions. *J. Hazard. Mater.* **351**, 224–231 (2018).
35. Kingma, A. J. Compatibility of nonionic surfactants with membrane materials and their cleaning performance. *Food Bioprod. Process.* **93**, 304–309 (2015).
36. Alpatova, A. et al. In situ conductive spacers for early pore wetting detection in membrane distillation. *Sep. Purif. Technol.* **294**, 121162 (2022).
37. Hakim, A., Suzuki, T. & Kobayashi, M. Strength of humic acid aggregates: effects of divalent cations and solution pH. *ACS Omega* **4**, 8559–8567 (2019).
38. Hart, J. R. *Ethylenediaminetetraacetic Acid and Related Chelating Agents*. (Ullmann's Encyclopedia of Industrial Chemistry, 2000).
39. Peng, Y., Ge, J., Li, Z. & Wang, S. Effects of anti-scaling and cleaning chemicals on membrane scale in direct contact membrane distillation process for RO brine concentrate. *Sep. Purif. Technol.* **154**, 22–26 (2015).
40. Charfi, A., Kim, S., Yoon, Y. & Cho, J. Optimal cleaning strategy to alleviate fouling in membrane distillation process to treat anaerobic digestate. *Chemosphere* **279**, 130524 (2021).
41. Guillen-Burrieza, E., Ruiz-Aguirre, A., Zaragoza, G. & Arafat, H. A. Membrane fouling and cleaning in long term plant-scale membrane distillation operations. *J. Membr. Sci.* **468**, 360–372 (2014).
42. Dow, N. et al. Demonstration of membrane distillation on textile waste water: assessment of long term performance, membrane cleaning and waste heat integration. *Environ. Sci. Water Res. Technol.* **3**, 433–449 (2017).
43. Jaishankar, J. & Srivastava, P. Molecular basis of stationary phase survival and applications. *Front Microbiol* **8**, 2000 (2017).
44. Goh, S., Zhang, J., Liu, Y. & Fane, A. G. Fouling and wetting in membrane distillation (MD) and MD-bioreactor (MDBR) for wastewater reclamation. *Desalination* **323**, 39–47 (2013).
45. Hermia, J. Constant pressure blocking filtration law application to powder-law non-Newtonian fluid. *Trans. Inst. Chem. Eng.* **60**, 183–187 (1982).
46. Crittenden, J. *Water Treatment: Principles and Design*. (John Willey & Sons, Inc, 2005).
47. Javier, L., Farhat, N. M. & Vrouwenvelder, J. S. Enhanced hydraulic cleanability of biofilms developed under a low phosphorus concentration in reverse osmosis membrane systems. *Water Res. X* **10**, 100085 (2021).
48. Li, Q. & Elimelech, M. Organic fouling and chemical cleaning of nanofiltration membranes: Measurements and mechanisms. *Environ. Sci. Technol.* **38**, 4683–4693 (2004).
49. You, H. S., Huang, C. P., Pan, J. R. & Chang, S. C. Behavior of membrane scaling during crossflow filtration in the anaerobic MBR system. *Sep. Sci. Technol.* **41**, 1265–1278 (2006).
50. Alnajjar, H., Tabatabai, A., Alpatova, A., Leiknes, T. & Ghaffour, N. Organic fouling control in reverse osmosis (RO) by effective membrane cleaning using saturated CO2 solution. *Sep. Purif. Technol.* **264**, 118410 (2021).
51. Braccini, I. & Pérez, S. Molecular basis of Ca2+-induced gelation in alginates and pectins: the Egg-Box model revisited. *Biomacromolecules* **2**, 1089–1096 (2001).
52. Morel, F. M. & Hering, J. G. *Principles and Applications of Aquatic Chemistry*. (John Wiley & Sons, 1993).
53. Bagheri, M. & Mirbagheri, S. A. Critical review of fouling mitigation strategies in membrane bioreactors treating water and wastewater. *Bioresour. Technol.* **258**, 318–334 (2018).
54. Lee, E.-J. et al. Influence of sodium hypochlorite used for chemical enhanced backwashing on biophysical treatment in MBR. *Desalination* **316**, 104–109 (2013).
55. Vanysacker, L., Bernshtein, R. & Vankelecom, I. F. Effect of chemical cleaning and membrane aging on membrane biofouling using model organisms with increasing complexity. *J. Membr. Sci.* **457**, 19–28 (2014).
56. Goli, M., Pande, M. & Bellaloui, N. Effects of chelating agents on protein, oil, fatty acids, and minerals in soybean seed. *Agric. Sci.* **3**, 517–523 (2012).
57. Chen, W., Westerhoff, P., Leenheer, J. A. & Booksh, K. Fluorescence excitation −emission matrix regional integration to quantify spectra for dissolved organic matter. *Environ. Sci. Technol.* **37**, 5701–5710 (2003).
58. Coble, P., Spencer, R. G. M., Baker, A. & Reynolds, D. *Aquatic Organic Matter Fluorescence*. (Cambridge University Press, 2014).

59. Simon, M. & Azam, F. Protein content and protein synthesis rates of planktonic marine bacteria. *Mar. Ecol. Prog. Ser.* **51**, 201–213 (1989).
60. Wang, Z., Wu, Z. & Tang, S. Characterization of dissolved organic matter in a submerged membrane bioreactor by using three-dimensional excitation and emission matrix fluorescence spectroscopy. *Water Res.* **43**, 1533–1540 (2009).
61. Hobley, L., Harkins, C., MacPhee, C. E. & Stanley-Wall, N. R. Giving structure to the biofilm matrix: An overview of individual strategies and emerging common themes. *FEMS Microbiol. Rev.* **39**, 649–669 (2015).
62. Kelly, S. T. & Zydney, A. L. Mechanisms for BSA fouling during microfiltration. *J. Membr. Sci.* **107**, 115–127 (1995).
63. Bao, X.-L., Lv, Y., Yang, B.-C., Ren, C.-G. & Guo, S.-T. A Study of the soluble complexes formed during calcium binding by soybean protein hydrolysates. *J. Food Sci.* **73**, C117–C121 (2008).
64. Iglesias, A., López, R., Fiol, S., Antelo, J. M. & Arce, F. Analysis of copper and calcium–fulvic acid complexation and competition effects. *Water Res.* **37**, 3749–3755 (2003).
65. Mikutta, R., Kleber, M., Kaiser, K. & Jahn, R. Review: Organic matter removal from soils using hydrogen peroxide, sodium hypochlorite, and disodium peroxodisulfate. *Soil Sci. Soc. Am. J.* **69**, 120–135 (2005).
66. Thurman, E. M., Wershaw, R. L., Malcolm, R. L. & Pinckney, D. J. Molecular size of aquatic humic substances. *Org. Geochem.* **4**, 27–35 (1982).
67. Goh, S. et al. Impact of a biofouling layer on the vapor pressure driving force and performance of a membrane distillation process. *J. Membr. Sci.* **438**, 140–152 (2013).
68. Chong, T. H., Wong, F. S. & Fane, A. G. The effect of imposed flux on biofouling in reverse osmosis: Role of concentration polarisation and biofilm enhanced osmotic pressure phenomena. *J. Membr. Sci.* **325**, 840–850 (2008).
69. Dreszer, C. et al. Hydraulic resistance of biofilms. *J. Membr. Sci.* **429**, 436–447 (2013).
70. Goh, S., Zhang, J., Liu, Y. & Fane, A. G. Membrane distillation bioreactor (MDBR)—a lower green-house-gas (GHG) option for industrial wastewater reclamation. *Chemosphere* **140**, 129–142 (2015).
71. Andrés-Mañas, J. A., Ruiz-Aguirre, A., Acién, F. G. & Zaragoza, G. Assessment of a pilot system for seawater desalination based on vacuum multi-effect membrane distillation with enhanced heat recovery. *Desalination* **443**, 110–121 (2018).
72. Duong, H. C., Duke, M., Gray, S., Cooper, P. & Nghiem, L. D. Membrane scaling and prevention techniques during seawater desalination by air gap membrane distillation. *Desalination* **397**, 92–100 (2016).
73. Castillo, E. H. C. et al. 3D printed spacers for organic fouling mitigation in membrane distillation. *J. Membr. Sci.* **581**, 331–343 (2019).
74. Duong, H. C., Gray, S., Duke, M., Cath, T. Y. & Nghiem, L. D. Scaling control during membrane distillation of coal seam gas reverse osmosis brine. *J. Membr. Sci.* **493**, 673–682 (2015).
75. Soukane, S., Naceur, M. W., Francis, L., Alsaadi, A. & Ghaffour, N. Effect of feed flow pattern on the distribution of permeate fluxes in desalination by direct contact membrane distillation. *Desalination* **418**, 43–59 (2017).
76. Rabuni, M. F., Nik Sulaiman, N. M., Aroua, M. K., Yern Chee, C. & Awanis Hashim, N. Impact of in situ physical and chemical cleaning on PVDF membrane properties and performances. *Chem. Eng. Sci.* **122**, 426–435 (2015).
77. Van Nevel, S., Koetzsch, S., Weilenmann, H.-U., Boon, N. & Hammes, F. Routine bacterial analysis with automated flow cytometry. *J. Microbiol. Methods* **94**, 73–76 (2013).
78. Prest, E. I., Hammes, F., Kötzsch, S., van Loosdrecht, M. C. M. & Vrouwenvelder, J. S. Monitoring microbiological changes in drinking water systems using a fast and reproducible flow cytometric method. *Water Res.* **47**, 7131–7142 (2013).
79. Liu, H. & Fang, H. H. Extraction of extracellular polymeric substances (EPS) of sludges. *J. Biotechnol.* **95**, 249–256 (2002).
80. Jang, Y. et al. Colloidal silica fouling mechanism in direct-contact membrane distillation. *Desalination* **527**, 115554 (2022).
81. Blankert, B., Betlem, B. H. L. & Roffel, B. Dynamic optimization of a dead-end filtration trajectory: Blocking filtration laws. *J. Membr. Sci.* **285**, 90–95 (2006).
82. Al-juboori, R. A. et al. Power effect of ultrasonically vibrated spacers in air gap membrane distillation: Theoretical and experimental investigations. *Sep. Purif. Technol.* **262**, 118319 (2021).

ACKNOWLEDGEMENTS

This study was supported by King Abdullah University of Science and Technology (KAUST), Saudi Arabia. The authors acknowledge help, assistance, and support from the Water Desalination and Reuse Center (WDRC) and KAUST staff.

AUTHOR CONTRIBUTIONS

The manuscript was written with the contributions of all authors. N.A.A.: conceptualization, methodology, investigation, data curation, formal analysis, visualization, writing—original draft, writing—review and editing. H.E.: conceptualization, methodology, investigation, data curation, formal analysis, visualization, writing—original draft, writing—review and editing. A.A.: conceptualization, methodology, investigation, formal analysis, writing—original draft, writing—review and editing. G.G.G.: methodology, writing—review and editing. B.B.: methodology, writing—review and editing. N.F.: methodology, writing—review and editing. J.S.V.: investigation, writing—review and editing. N.G.: conceptualization, methodology, investigation, formal analysis, writing—review and editing, supervision. All authors read and approved the final manuscript.

COMPETING INTERESTS

The authors declare no competing interests.

ADDITIONAL INFORMATION

Correspondence and requests for materials should be addressed to Noreddine Ghaffour.